

Semiclassical Analysis of the 3d/3d Relation

Yuji Terashima¹ and Masahito Yamazaki²

¹Department of Mathematics, Tokyo Institute of Technology, Tokyo 152-8551, Japan

²Princeton Center for Theoretical Science, Princeton University, NJ 08544, USA

Abstract

We provide quantitative evidence for our previous conjecture which states an equivalence of the partition function of a 3d $\mathcal{N} = 2$ gauge theory on a duality wall and that of the $SL(2, \mathbb{R})$ Chern-Simons theory on a mapping torus, for a class of examples associated with once-punctured torus. In particular, we demonstrate that a limit of the 3d $\mathcal{N} = 2$ partition function reproduces the hyperbolic volume and the Chern-Simons invariant of the mapping torus. This is shown by analyzing the classical limit of the trace of an element of the mapping class group in the Hilbert space of the quantum Teichmüller theory. We also show that the subleading correction to the partition function reproduces the Reidemeister torsion.

1 Introduction

In our previous paper [1], based on previous works [2, 3] we proposed an equivalence of the partition functions of two 3d theories: one is a 3d supersymmetric $\mathcal{N} = 2$ theory on a squashed 3-sphere S_b^3 , where the 3d theory is realized as a duality 1/2 BPS domain wall inside a 4d $\mathcal{N} = 2$ theory; another is the 3d bosonic $SL(2, \mathbb{R})$ Chern-Simons theory defined on a mapping torus M_3 .¹ Schematically, our relation is written as

$$Z_{\text{3d } \mathcal{N}=2 \text{ theory}}[S_b^3] = Z_{\text{3d } SL(2, \mathbb{R}) \text{ CS}}[M_3], \quad (1.1)$$

where the parameter b is related to the level k of the Chern-Simons theory.² This relation should arise from the dimensional reduction of the 6d $(2, 0)$ theory on $S^3 \times M_3$, and is a 3d/3d counterpart of the 4d/2d correspondence (AGT conjecture) [4]. See [5] for a recent discussion, and [6, 7, 8] for related proposals.

In [1], we outlined the derivation of the relation (1.1) using a chain of connections with quantum Liouville and Teichmüller theories. While suggestive, this argument should not be regarded as a proof, since it relies on several conjectures existing in the literature. It is therefore highly desirable to provide more quantitative evidence for this conjecture.

In this paper we perform quantitative checks of our proposal in the example of the once-punctured torus. In particular, we are going to show that the $b \rightarrow 0$ limit (which is the classical limit $k \rightarrow \infty$ of the $SL(2, \mathbb{R})$ Chern-Simons theory) of the partition function of 3d $\mathcal{N} = 2$ theories reproduces the hyperbolic volume and the Chern-Simons invariant³ of the mapping torus:

$$Z_{\text{3d } \mathcal{N}=2 \text{ theory}}[S_b^3] \rightarrow \exp \left[\frac{1}{2\pi b^2} (\text{Vol}(M_3) + 2\pi^2 i \text{CS}(M_3)) \right], \quad \text{when } b \rightarrow 0. \quad (1.2)$$

Since the right hand side is known to be the classical limit of the partition function of $SL(2, \mathbb{R})$ Chern-Simons theory on M_3 [9], (1.2) is nothing but the $b \rightarrow 0$ limit of (1.1).

The rest of the paper is organized as follows. In section 2, we summarize in more detail the results of this paper. In section 3 we study the semiclassical limit of the right hand side of (1.1) as a trace in quantum Teichmüller theory. The result is then shown to be equivalent to

¹In [1], we considered two possibilities: M_3 is either $\Sigma \times I$ or a mapping torus. In this paper we focus on the latter.

²More precisely, the right hand side should be defined by a path integral over the Teichmüller component of the moduli space of flat connections. Such a subtlety, however, does not play a role in the semiclassical analysis of this paper.

³This is an invariant of a hyperbolic 3-manifold, and takes values in real numbers modulo half-integers.

the geometric potential for hyperbolic volume. We conclude in section 4 with short remarks. We also include several appendices on quantum dilogarithm and hyperbolic geometry.

2 Summary of Results

Let us first summarize the main results of the paper in more detail.

In the case of the once-punctured torus, the corresponding 3d $\mathcal{N} = 2$ theories and their partition functions has been described in section 4 of [1]; the gauge theory is a quiver gauge theory where the $T[SU(2)]$ theory (and mass deformation thereof) is glued together by gauging global symmetries, with Chern-Simons terms added for the corresponding gauge fields.

The important result here, which is first proposed in [2], worked out concretely in [3] and discussed in more generally in [1], is that the 3d $\mathcal{N} = 2$ partition function coincides with an expectation value of an operator in quantum Teichmüller theory.⁴ Given a punctured Riemann surface Σ , Teichmüller theory gives an associated Hilbert space $\mathcal{H}_T(\Sigma)$, together with an action of an element φ of the mapping class group of Σ . We can then define a trace of φ in the Hilbert space, and this coincides with the partition function of the 3d $\mathcal{N} = 2$ theory:

$$Z_{\text{3d } \mathcal{N}=2 \text{ theory}}[S_b^3] = \text{Tr}_{\mathcal{H}_T(\Sigma)}(\varphi) . \quad (2.1)$$

We are going to analyze the semiclassical limit of our trace $\text{Tr}(\varphi)$. The result is given by

$$\text{Tr}(\varphi) \rightarrow \int dx dy du dv \exp \left[\frac{1}{2\pi i b^2} V_{\text{trace}}(x, y, u, v; h) \right] , \quad (2.2)$$

where x, y, u, v are a set of parameters and h is a parameter associated with the puncture of Σ , and corresponds to a mass parameter in 3d $\mathcal{N} = 2$ theory. V_{trace} is quadratic with respect to u and v , and after extremizing with respect to these variables, we have a function $V_{\text{trace}}(x, y; h)$:

$$\text{Tr}(\varphi) \rightarrow \int dx dy \exp \left[\frac{1}{2\pi i b^2} V_{\text{trace}}(x, y; h) \right] . \quad (2.3)$$

We will find that this is a linear function with respect to h .

⁴As explained in [1], this statement is not yet completely justified when we need to glue two theories by gauging global symmetries of the Coulomb branch, which are quantum symmetries of the theory.

Let us now describe the other side of (1.1). The mapping torus is a 3-manifold defined from Σ and φ . In particular, when φ satisfies $|\text{tr}(\varphi)| > 2$, M_3 admits a finite volume, complete hyperbolic metric [10]. We can triangulate M_3 into ideal tetrahedra. The shape of each ideal tetrahedron is specified by a parameter called the modulus of the tetrahedron, and these parameters should satisfy a set of consistency conditions. These conditions are generated from the derivatives of a single potential V_{geom} [11]. At the extremal point this potential reproduces the combination $\text{Vol}(M_3) + 2\pi^2 i \text{CS}(M_3)$ of the 3-manifold M_3 .

We will demonstrate two facts. First, we show (up to constant terms)

$$V_{\text{trace}} \Big|_{h=0} = V_{\text{geom}} , \quad (2.4)$$

where we have identified the parameters x, y of (2.3) with the moduli of tetrahedra. This in particular implies (1.2) for $h = 0$, since the hyperbolic volume (plus the Chern-Simons invariant) is given by the critical value of V_{geom} .

Second, for $h \neq 0$ we show that

$$V_{\text{trace}}(x, y; h) = V_{\text{geom}}(x, y; h) , \quad (2.5)$$

where the potential $V_{\text{geom}}(x, y; h)$ gives a 1-parameter deformation of hyperbolic structure [12]. The parameter h is identified with the longitude parameter \mathfrak{l} , and serves as a Lagrange multiplier⁵. Its dual variable, the meridian parameter \mathfrak{m} , is given by

$$\mathfrak{m} = \frac{\partial V_{\text{geom}}}{\partial h} . \quad (2.6)$$

By using this equation we can eliminate one of the variables x, y from V_{trace} , and the result is a potential depending on \mathfrak{m} . By Extremizing this potential, we recover a polynomial in $e^{\mathfrak{m}}$ and $e^{\mathfrak{l}}$, the A-polynomial [13] of the mapping torus.

We also analyze subleading contributions to our trace and find that it reproduces the Reidemeister(-Ray-Singer) torsion of the 3-manifold, which is the 1-loop contribution in the Chern-Simons theory [14].

We stress we do not need to invoke any conjectures in the logic given above⁶; for example, we do not need to assume AGT conjecture nor the equivalence of quantum Liouville theory and quantum Teichmüller theory. The partition function of our 3d $\mathcal{N} = 2$ theory is computed

⁵We would like to thank T. Dimofte for suggesting the possibility that the puncture parameter is the longitude parameter.

⁶See the comment in footnote 4, however.

exactly by localization, and we can analyze its semiclassical limit without any ambiguity. The only fact we need is that the partition function can be expressed as an expectation value of an operator in a certain well-defined Hilbert space, which is our case is the quantum Teichmüller space. This naturally realizes the change of variables⁷ needed for direct comparison with hyperbolic volume.

3 Semiclassical Limit of the Trace

We are going to describe the semiclassical limit of our trace in quantum Teichmüller theory.

The Hilbert space of the quantum Teichmüller theory for the once-punctured torus (see section 4.3 of [1]) is spanned by \mathbf{x}, \mathbf{y} and \mathbf{z} , whose non-trivial commutation relations are given by

$$[\mathbf{x}, \mathbf{y}] = [\mathbf{y}, \mathbf{z}] = [\mathbf{z}, \mathbf{x}] = -4\pi i b^2, \quad (3.1)$$

or equivalently

$$\mathbf{X}\mathbf{Y} = q^{-4}\mathbf{Y}\mathbf{X}, \quad \mathbf{Y}\mathbf{Z} = q^{-4}\mathbf{Z}\mathbf{Y}, \quad \mathbf{Z}\mathbf{X} = q^{-4}\mathbf{X}\mathbf{Z}, \quad (3.2)$$

where in the following capitalized variables represent exponentiation,

$$\mathbf{X} = e^{\mathbf{x}}, \quad \mathbf{Y} = e^{\mathbf{y}}, \quad \mathbf{Z} = e^{\mathbf{z}}, \quad (3.3)$$

and $q := e^{i\pi b^2}$. This algebra has a central element, i.e. a constant, corresponding to the size of the hole

$$h := \mathbf{x} + \mathbf{y} + \mathbf{z}. \quad (3.4)$$

There are 2 remaining variables \mathbf{x} and \mathbf{y} , and we can choose a basis $|x\rangle$ such that

$$\mathbf{x}|x\rangle = x|x\rangle, \quad \mathbf{y}|x\rangle = 4\pi i b^2 \frac{\partial}{\partial x}|x\rangle. \quad (3.5)$$

This is a complete set

$$\int dx |x\rangle \langle x| = 1. \quad (3.6)$$

⁷This refers to the change between Fock coordinates and Fenchel-Nielsen coordinates.

Similarly, we can choose a different basis $|y\rangle$. This again spans a complete set.

The mapping class group $SL(2, \mathbb{Z})$ acts on this Hilbert space. For this purpose it is useful to choose the generators of $SL(2, \mathbb{Z})$:

$$L = \begin{pmatrix} 1 & 1 \\ 0 & 1 \end{pmatrix}, \quad R = \begin{pmatrix} 1 & 0 \\ 1 & 1 \end{pmatrix}. \quad (3.7)$$

As explained in [1], the action of L has the effect

$$\begin{aligned} X &\rightarrow L^{-1} X L = (1 + qX^{-1})^{-1}(1 + q^3X^{-1})^{-1}Z, \\ Y &\rightarrow L^{-1} Y L = (1 + qX)(1 + q^3X)Y, \\ Z &\rightarrow L^{-1} Z L = X^{-1}, \end{aligned} \quad (3.8)$$

This preserves the commutation relations given in (3.1). The operator L , representing an action of L in $SL(2, \mathbb{Z})$, can be written as a product of two operators⁸

$$L = L(X, Z) = f_L(e^{x+z})g_L(X) = f_L(q^{-2}XZ)g_L(X), \quad (3.9)$$

where $f_L(e^{x+z})$ and $g_L(X)$ are given by

$$f_L(e^{x+z}) = \exp \left[\frac{1}{8\pi i b^2} (x+z)^2 \right], \quad g_L(X) = e_b \left(\frac{x}{2\pi b} \right)^{-1}, \quad (3.10)$$

where $e_b(z)$ is the quantum dilogarithm function defined in Appendix A. These functions satisfy (see (A.7))

$$f_L(q^4 X) = X f_L(X), \quad g_L(q^4 X) = (1 + qX)(1 + q^3 X)g_L(X). \quad (3.11)$$

Note that in the convention here the operator $f_L(q^{-2}XZ)$ acts first, then $g_L(X)$. Conjugation by $f_L(q^{-2}XZ)$ acts as

$$X \rightarrow q^{-4}X^2Z, \quad Y \rightarrow Y, \quad Z \rightarrow X^{-1}, \quad (3.12)$$

whereas the conjugation by $g_L(X)$ as

$$X \rightarrow X, \quad Y \rightarrow (1 + qX)(1 + q^3X)Y, \quad Z \rightarrow (1 + q^{-1}X)^{-1}(1 + q^{-3}X)^{-1}Z, \quad (3.13)$$

⁸Essentially the same decomposition can be found in [15].

and we can verify that the composition of the two gives the desired result (3.8).

Similarly, R is given by⁹

$$R = R(Y, Z) = f_R(e^{y+z})g_R(Y) = f_R(q^2YZ)g_R(Y), \quad (3.14)$$

where f_R and g_R are given by

$$f_R(e^{y+z}) = \exp \left[-\frac{1}{8\pi i b^2} (y+z)^2 \right], \quad g_R(Y) = e_b \left(-\frac{y}{2\pi b} \right). \quad (3.15)$$

In general an element of the mapping class group is obtained as a product of these two operators. Namely, when we have $\varphi = L^{n_1} R^{m_1} L^{n_2} R^{m_2} \dots$, we have¹⁰

$$\varphi | \rangle = \dots R(Y, Z)^{m_2} L(X, Z)^{n_2} R(Y, Z)^{m_1} L(X, Z)^{n_1} | \rangle. \quad (3.18)$$

3.1 Examples: $\varphi = LR$

Let us now discuss concrete examples. For $\varphi = LR$, the mapping torus is given by the complement of the figure eight knot. The trace is given by

$$\text{Tr}(\varphi) = \int dx \langle x | f_R(h - x) g_R(y) f_L(h - y) g_L(x) | x \rangle.$$

By inserting a complete set as in

$$R \underbrace{\hspace{1cm}}_y L \underbrace{\hspace{1cm}}^x,$$

⁹For this purpose it is useful to note that the commutation relations are invariant under the simultaneous exchange of X, Y and q, q^{-1} .

¹⁰Let us comment on the ordering of operators. As an example, $\varphi = LR$ is represented by

$$\varphi = L(X, Z) R(L^{-1}YL, L^{-1}ZL). \quad (3.16)$$

Note that in this expression the argument inside R is conjugated by an action of L . This is because the second operator R should act on transformed variables $L^{-1}YL$ and $L^{-1}ZL$, rather than the original variables. However, this expression is equivalent to

$$\varphi = R(Y, Z) L(X, Z). \quad (3.17)$$

This means that in the Schrödinger representation all we need to do is to multiply the ket vector from the left (meaning we read the operators from right to left), while keeping the arguments for the operators to be the same variables X, Y and Z .

this is computed to be

$$\begin{aligned}\mathrm{Tr}(\varphi) &= \int dx dy \langle x | f_R(h - x) g_R(y) | y \rangle \langle y | f_L(h - y) g_L(x) | x \rangle \\ &= \int dx dy f_R(h - x) g_R(y) f_L(h - y) g_L(x).\end{aligned}$$

Let us study the classical limit $b \rightarrow 0$ of this quantity. In this limit, the functions $g_L(x)$ and $g_R(y)$ simplifies to (see (A.2))

$$g_L(x) \rightarrow \exp \left[-\frac{1}{2\pi i b^2} \mathrm{Li}_2(-e^x) \right], \quad g_R(x) \rightarrow \exp \left[\frac{1}{2\pi i b^2} \mathrm{Li}_2(-e^{-x}) \right], \quad (3.19)$$

and similarly for $f_R(x)$ and $g_R(x)$. Therefore, the classical limit is given by

$$\mathrm{Tr}(\varphi) \rightarrow \int dx dy \exp \left[\frac{1}{2\pi i b^2} V_{\mathrm{trace}}(x, y; h) \right], \quad (3.20)$$

where

$$V_{\mathrm{trace}}(x, y; h) = -\mathrm{Li}_2(-e^x) - \frac{1}{4}(h - x)^2 + \mathrm{Li}_2(-e^{-y}) + \frac{1}{4}(h - y)^2. \quad (3.21)$$

Note that the quadratic part of h cancel out in this expression. As we will see, this is a generic feature of the potential in the example of the once-punctured torus bundles discussed in this paper.

Let temporarily set $h = 0$. By extremizing $V_{\mathrm{trace}}|_{h=0}$, we have

$$\frac{1}{1 + e^x} = e^{-x/2}, \quad \frac{1}{1 + e^{-y}} = e^{+y/2}, \quad (3.22)$$

and the potential is maximized at $e^x = e^y = \frac{-1+i\sqrt{3}}{2}$. The value of the potential there is given by $\mathrm{Li}_2(-e^{2\pi i/3}) - \mathrm{Li}_2(-e^{-2\pi i/3})$, whose imaginary (real) part gives the hyperbolic volume (Chern-Simons invariant) of the figure eight knot complement!

$$\mathrm{Vol}(4_1) = 2.02988..., \quad \mathrm{CS}(4_1) = 0. \quad (3.23)$$

This is not a coincidence, and we will present a general proof of this statement in sections 3.3 and 3.4. The discussion below serves as an illustrative example.

Let us choose the so-called canonical triangulation [16] of the figure eight knot complement. In this triangulation we have two ideal tetrahedra, and in the parametrization of [17]

their moduli are parametrized by two parameters x and y (see Figure 1, with $h = 0$). The consistency conditions for x, y are given by

$$e^{-x/2} = \frac{1}{1 - e^{-(i\pi-x)}}, \quad e^{-y/2} = \frac{1}{1 - e^{-(i\pi-y)}}, \quad (3.24)$$

which coincides with (3.22). This shows that V_{trace} coincides with the V_{geom} (up to constant terms).

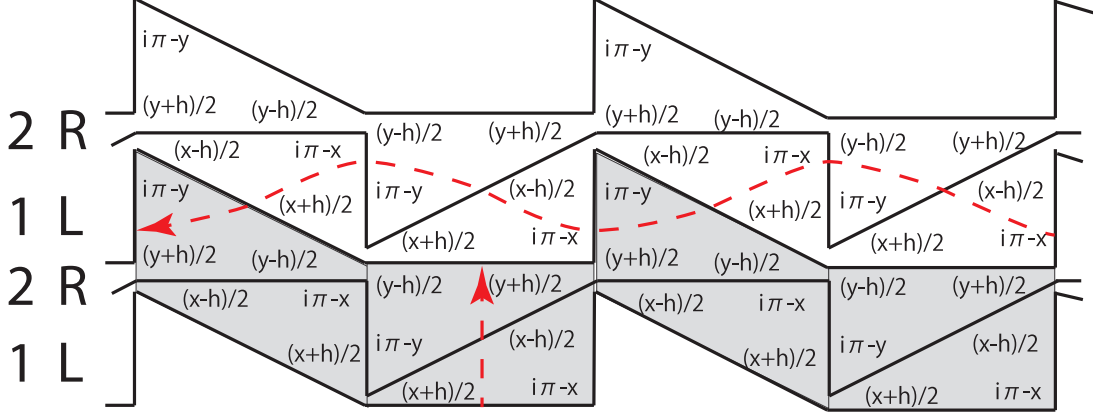


Figure 1: The boundary torus for canonical triangulation of the figure eight knot complement. The gray region represents the fundamental region of the torus, and the each of the two strips (consisting of four triangles) represents the boundary of a tetrahedron. The modulus of the tetrahedra are parametrized by two complex numbers x and y . The horizontal (vertical) dotted arrow represents the longitude (meridian) of the torus.

Let us next discuss the h -dependence of the potential. Extremizing the potential, we have

$$\frac{1}{1 + e^x} = e^{-(x-h)/2}, \quad \frac{1}{1 + e^{-y}} = e^{(y-h)/2}, \quad (3.25)$$

This is reproduced from the parametrization as in Figure 1. This 1-parameter deformation preserve the gluing conditions around the edges of tetrahedra, but the longitude parameter is deformed to be ¹¹

$$\mathfrak{l} = -(x - h)/2 + (i\pi - y) + (x + h)/2 - (i\pi - y) + i\pi = h + i\pi. \quad (3.26)$$

This is the 1-parameter deformation of the hyperbolic structure considered in [12]. The

¹¹The complete hyperbolic metric corresponds to $\mathfrak{l} = i\pi$.

meridian parameter is given by

$$\mathbf{m} = (x + h)/2 - (y + h)/2 = (x - y)/2 = \frac{\partial V_{\text{trace}}(x, y; h)}{\partial h} = \frac{\partial V_{\text{trace}}(x, y; \mathfrak{l})}{\partial \mathfrak{l}}. \quad (3.27)$$

Note that this is independent of h .

Eliminating the variable y using (3.27), the potential becomes

$$V_{\text{trace}}(x; \mathbf{m}) = -\text{Li}_2(-e^x) + \text{Li}_2(-e^{-(x-2\mathbf{m})}) - \frac{1}{4}(x^2 - (x - 2\mathbf{m})^2) + (\mathfrak{l} - i\pi)\mathbf{m}. \quad (3.28)$$

By extremizing this potential with respect to x and \mathbf{m} and eliminating the variable x , we have a polynomial equation with respect to $L := e^{\mathfrak{l}}$ and $M := e^{\mathbf{m}}$:

$$A(L, M) = 1 + L(-M^{-2} + M^{-1} + 2 + M - M^2) + L^2. \quad (3.29)$$

This coincides with the known expression for the A-polynomial of the figure eight knot complement.

We can refine our analysis by going to next order, by evaluating Gaussian integral of the potential $V_{\text{trace}}(x; \mathbf{m})$ around the saddle point. Explicit computation verifies that this is given by $\sqrt{T(\mathbf{m})}$, where $T(\mathbf{m})$ is given by

$$\frac{1}{\sqrt{(M^2 - 3M + 1)(M^2 + M + 1)}/M} = \frac{1}{\sqrt{(2 \cosh \mathbf{m} - 3)(2 \cosh \mathbf{m} + 1)}}. \quad (3.30)$$

This coincides (up to multiplication by an overall constant) with the Reidemeister torsion for the figure eight knot complement [18].

3.2 Example: $\varphi = L^2 R$

Let us next discuss the example of $\varphi = L^2 R$. By inserting a complete set as in

$$R \underbrace{\quad}_{y_1} L \underbrace{\quad}_{x_2, u_2} L \underbrace{\quad}_{x_3},$$

The trace is computed to be

$$\begin{aligned}
\text{Tr}(\varphi) &= \int dy_1 dx_2 du_2 dx_3 \langle x_3 | f_R(h - \mathbf{x}) g_R(\mathbf{y}) | y_1 \rangle \langle y_1 | f_L(h - \mathbf{y}) g_L(\mathbf{x}) | x_2 \rangle \\
&\quad \times \langle x_2 | u_2 \rangle \langle u_2 | f_L(h - \mathbf{y}) g_L(\mathbf{x}) | x_3 \rangle \\
&= \int dy_1 dx_2 du_2 dx_3 f_R(h - x_3) g_R(y_1) f_L(h - y_1) g_L(x_2) f_L(h - u_2) g_L(x_3) \\
&\quad \times \exp \left[\frac{1}{4\pi i b^2} (x_3 y_1 - y_1 x_2 + x_2 u_2 - u_2 x_3) \right].
\end{aligned}$$

The classical limit is given by

$$\text{Tr}(\varphi) \rightarrow \int dy_1 dx_2 du_2 dx_3 \exp \left[\frac{1}{2\pi i b^2} V_{\text{trace}}(y_1, x_2, u_2, x_3; h) \right], \quad (3.31)$$

where

$$\begin{aligned}
V_{\text{trace}}(y_1, x_2, u_2, x_3; h) &= -\frac{1}{4}(h - x_3)^2 + \text{Li}_2(-e^{-y_1}) + \frac{1}{4}(h - y_1)^2 - \text{Li}_2(-e^{x_2}) \\
&\quad + \frac{1}{4}(h - u_2)^2 - \text{Li}_2(-e^{x_3}) + \frac{1}{2}(x_3 y_1 - y_1 x_2 + x_2 u_2 - u_2 x_3).
\end{aligned} \quad (3.32)$$

The resulting expression is quadratic in u_2 , so we can easily integrate out u_2 , giving

$$\begin{aligned}
V_{\text{trace}}(y_1, x_2, x_3; h) &= -\text{Li}_2(-e^{x_3}) - \text{Li}_2(-e^{x_2}) + \text{Li}_2(-e^{-y_1}) - \frac{1}{4}x_3^2 + \frac{1}{4}y_1^2 \\
&\quad - \frac{1}{4}(x_3 - x_2)^2 + \frac{1}{2}(x_3 y_1 - y_1 x_2) + \frac{1}{2}h(x_2 - y_1).
\end{aligned} \quad (3.33)$$

Note again that this has a linear dependence with respect to h .

When we take $h = 0$, the potential is maximized by

$$e^{x_3} = \frac{-3 + i\sqrt{7}}{8}, \quad e^{x_2} = e^{y_1} = \frac{-1 + i\sqrt{7}}{4}, \quad (3.34)$$

and the imaginary part of the extremal value of the potential coincides with the volume of the mapping torus, which is known to be 2.66674... . The real part, divided by a factor $2\pi^2$ (see (1.2)), gives the Chern-Simons invariant -0.02083 .

From the h -linear part, the meridian variable is defined by

$$\mathfrak{m} = \frac{\partial V_{\text{trace}}(y_1, x_2, x_3; h)}{\partial h} = \frac{1}{2}(x_2 - y_1), \quad (3.35)$$

and procedures similar to the previous example give

$$L^2 M + L(-1/M + 2 + 2M - M^2) + 1 = 0, \quad (3.36)$$

which is the known expression for the A-polynomial. The Gaussian integral around the saddle point is computed to be $\sqrt{T(\mathbf{m})}$ with

$$T(\mathbf{m}) = \frac{1}{\sqrt{1 + M(1 + M)(-2 - 3M + M^2)/M}} = \frac{1}{\sqrt{4 \cosh \mathbf{m}^2 - 4 \cosh \mathbf{m} - 7}}. \quad (3.37)$$

This again coincides with the Reidemeister torsion [18].

3.3 General φ : Computation of the Trace

Let us finally discuss the case of a general element φ in the mapping class group.

The element φ is represented as a word of L and R , and its trace is again computed by inserting a complete basis of states between L 's and R 's. Depending on the four possibilities, we are going to insert complete sets as in

$$\cdots L \underbrace{\quad}_{x_k, u_k} L \cdots, \quad \cdots R \underbrace{\quad}_{y_k, v_k} R \cdots, \quad \cdots L \underbrace{\quad}_{x_k} R \cdots, \quad \cdots R \underbrace{\quad}_{y_k} L \cdots.$$

For example, for $\varphi = \text{LLLRRLRR}$, we have

$$L \underbrace{\quad}_{x_1, u_1} L \underbrace{\quad}_{x_2, u_2} L \underbrace{\quad}_{x_3} R \underbrace{\quad}_{y_4, v_4} R \underbrace{\quad}_{y_5} L \underbrace{\quad}_{x_6} R \underbrace{\quad}_{y_7, v_7} R \underbrace{\quad}_{y_8}.$$

This gives a potential $V_{\text{trace}}(x, y, u, v; h)$, which after integrating out u and v reduces to the potential $V_{\text{trace}}(x, y; h)$. In the following we will determine the x_k and y_k dependence of the potential $V_{\text{trace}}(x, y; h)$. For this purpose we discuss $2^3 = 8$ possibilities separately. The symbol \equiv means equality up to terms independent of x_k or y_k .

In the first four cases, we concentrate on the x_k dependence of the potential.

1. Suppose we have $\cdots \text{LLL} \cdots$. We could then insert a complete set as in

$$\cdots L \underbrace{\quad}_{x_{k-1}, u_{k-1}} L \underbrace{\quad}_{x_k, u_k} L \underbrace{\quad}_{x_{k+1}} \cdots,$$

and then we have

$$V_{\text{trace}}(x, y, u, v; h) \equiv -\text{Li}_2(-e^{x_k}) + \frac{1}{4}((h - u_{k-1})^2 + (h - u_k)^2) \\ + \frac{1}{2}(x_{k-1}u_{k-1} - u_{k-1}x_k + x_k u_k - u_k x_{k+1}).$$

We can trivially integrate out u_{k-1} and u_k , and the potential becomes

$$V_{\text{trace}}(x, y; h) \equiv -\text{Li}_2(-e^{x_k}) + \frac{1}{4}(-2x_k^2) + \frac{1}{2}x_k(x_{k-1} + x_{k+1}). \quad (3.38)$$

2. For $\cdots \underbrace{\text{L}}_{x_{k-1}, u_{k-1}} \underbrace{\text{L}}_{x_k} \underbrace{\text{R}}^{y_{k+1}} \cdots$, we have

$$V_{\text{trace}}(x, y; h) \equiv -\text{Li}_2(-e^{x_k}) + \frac{1}{4}(-2x_k^2) + \frac{1}{2}x_k(x_{k-1} + y_{k+1}). \quad (3.39)$$

Note that this is the same as the previous answer except that x_{k+1} is replaced by y_{k+1} . The same remark applies to all the remaining cases, and each makes a pair with another.

3. The analysis is similar for other cases. For $\cdots \underbrace{\text{R}}^{y_{k-1}} \underbrace{\text{L}}_{x_k, u_k} \underbrace{\text{L}}_{x_{k+1}} \cdots$, we have

$$V_{\text{trace}}(x, y; h) \equiv -\text{Li}_2(-e^{x_k}) + \frac{1}{4}(-x_k^2) + \frac{1}{2}x_k(x_{k+1} - y_{k-1}) + \frac{h}{2}x_k. \quad (3.40)$$

4. For $\cdots \underbrace{\text{R}}^{y_{k-1}} \underbrace{\text{L}}_{x_k} \underbrace{\text{R}}_{y_{k+1}} \cdots$, we have

$$V_{\text{trace}}(x, y; h) \equiv -\text{Li}_2(-e^{x_k}) + \frac{1}{4}(-x_k^2) + \frac{1}{2}x_k(y_{k+1} - y_{k-1}) + \frac{h}{2}x_k. \quad (3.41)$$

The y_k dependence of the potential in the remaining four cases is determined similarly.

5. For $\cdots \underbrace{\text{R}}^{y_{k-1}, v_{k-1}} \underbrace{\text{R}}_{y_k, v_k} \underbrace{\text{R}}^{y_{k+1}} \cdots$, we have

$$V_{\text{trace}}(x, y; h) \equiv \text{Li}_2(-e^{-y_k}) + \frac{1}{4}(2y_k^2) + \frac{1}{2}y_k(-y_{k-1} - y_{k+1}). \quad (3.42)$$

6. For $\cdots \underbrace{\text{R}}^{y_{k-1}, v_{k-1}} \underbrace{\text{R}}_{y_k} \underbrace{\text{L}}_{x_{k+1}} \cdots$, we have

$$V_{\text{trace}}(x, y; h) \equiv \text{Li}_2(-e^{-y_k}) + \frac{1}{4}(2y_k^2) + \frac{1}{2}y_k(-y_{k-1} - x_{k+1}). \quad (3.43)$$

7. For $\cdots \underbrace{L}_{x_{k-1}} \underbrace{R^{y_k, v_k}}_{y_k} \underbrace{R^{y_{k+1}}}_{y_{k+1}} \cdots$, we have

$$V_{\text{trace}}(x, y; h) \equiv \text{Li}_2(-e^{-y_k}) + \frac{1}{4}y_k^2 + \frac{1}{2}y_k(x_{k-1} - y_{k+1}) + \frac{h}{2}(-y_k). \quad (3.44)$$

8. For $\cdots \underbrace{L}_{x_{k-1}} \underbrace{R^{y_k}}_{y_k} \underbrace{L^{x_{k+1}}}_{x_{k+1}} \cdots$, we have

$$V_{\text{trace}}(x, y; h) \equiv \text{Li}_2(-e^{-y_k}) + \frac{1}{4}y_k^2 + \frac{1}{2}y_k(x_{k-1} - x_{k+1}) + \frac{h}{2}(-y_k). \quad (3.45)$$

We have now determined the function $V_{\text{trace}}(x, y; h)$, since we know the dependence with respect to all the variables. In particular, we can extract the h -dependent part of the potential. For

$$L^{i_1} R^{j_1} L^{i_2} R^{j_2} \cdots L^{i_p} R^{j_p},$$

we can insert a complete set as in

$$\underbrace{L}_{x_1} \underbrace{L}_{x_2} \cdots \underbrace{L}_{x_{i_1-1}} \underbrace{L}_{x_{i_1}} \underbrace{R^{y_{i_1+1}}}_{y_{i_1+1}} \underbrace{R^{y_{i_1+2}}}_{y_{i_1+2}} \cdots \underbrace{R^{y_{i_1+j_1-1}}}_{y_{i_1+j_1-1}} \underbrace{R^{y_{i_1+j_1}}}_{y_{i_1+j_1}} \\ \underbrace{L}_{x_{i_1+j_1+1}} \underbrace{L}_{x_{i_1+j_1+2}} \cdots \underbrace{L}_{x_{i_1+j_1+i_2-1}} \underbrace{L}_{x_{i_1+j_1+i_2}} R \cdots,$$

(here we did not write u and v variables, which we integrate out anyway), and the h -dependent term of $V_{\text{trace}}(x, y; h)$ is

$$V_{\text{trace}} \supset \frac{h}{2} (x_1 + x_{i_1+1} + x_{i_1+i_2+1} + \cdots + x_{i_1+\dots i_{p-1}+1} \\ - y_1 - y_{j_1+1} - y_{j_1+j_2+1} - \cdots - y_{j_1+\dots j_{p-1}+1}). \quad (3.46)$$

3.4 General φ : Computation of Hyperbolic Volume

The 3-manifold discussed in this paper is a mapping torus of the once-punctured torus. This is a knot complement inside a 3-manifold, where the position of the knot corresponds to the puncture of the torus. There is a standard triangulation of the mapping torus, called the canonical triangulation [16]. This is treated in detail in a beautiful paper by Gueritaud [17].

As explained in [1], section 4.4, each L or R in the decomposition of φ corresponds to an ideal tetrahedron. The decomposition of φ into L and R represents how to stack these ideal tetrahedra Δ_k one by one.

The vertices of the ideal tetrahedron are at the puncture of the torus, so we need to cut the tetrahedron around the vertices. Since all the four vertices surround the same vertex,

the boundary of the tetrahedron around the puncture looks like a union of four triangles (see Figure 2). By repeating this for each tetrahedron we have a figure for the boundary torus. See Figure 3 for an example.

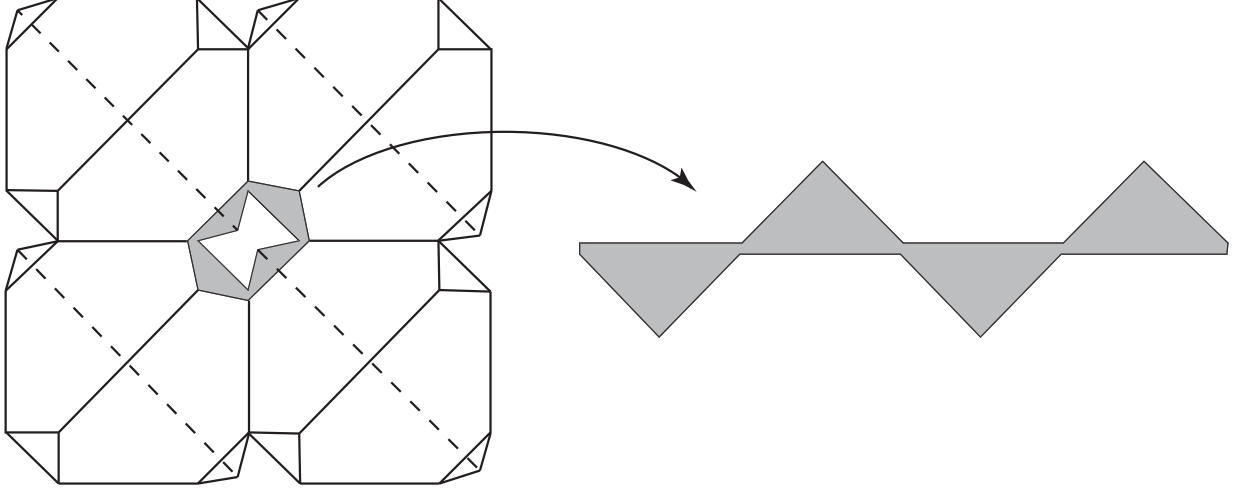


Figure 2: All the four vertices of an ideal tetrahedron gather around the puncture of the torus. When we cut the tetrahedron around a puncture, the boundary is a union of four triangles, colored gray.

An ideal tetrahedron has three dihedral angles (see Appendix B for this and related materials). We use a special parametrization of the dihedral angles due to [17]. This parametrization is given by following the two steps: first, we assign a variable w_k to each ideal tetrahedron Δ_k . Second, the shape parameters $e^{\alpha_k}, e^{\beta_k}, e^{\gamma_k}$ of Δ_k are given by the rules in Table 1, which depends on whether L or R is assigned to Δ_k and Δ_{k-1} , respectively.

Table 1: Parametrization of the dihedral angles in Δ_k . $\alpha_k, \beta_k, \gamma_k$ are (the logarithm of) the shape parameters of the tetrahedron Δ_k , see Figure 3. This is a 1-parameter deformation of the parametrization of [17]. We have changed the normalization of w_k ; w_k here is $2i$ times that in [17].

	$(\Delta_{k-1}, \Delta_k) = (L, L)$	$(\Delta_{k-1}, \Delta_k) = (R, R)$	$(\Delta_{k-1}, \Delta_k) = (L, R)$	$(\Delta_{k-1}, \Delta_k) = (R, L)$
α_k	$\frac{w_{k-1} + w_{k+1}}{2}$	$\frac{-w_{k-1} + 2w_k - w_{k+1}}{2}$	$\frac{w_{k-1} + w_k - w_{k+1} - h}{2}$	$\frac{-w_{k-1} + w_k + w_{k+1} + h}{2}$
β_k	$\frac{-w_{k-1} + 2w_k - w_{k+1}}{2}$	$\frac{w_{k-1} + w_{k+1}}{2}$	$\frac{-w_{k-1} + w_k + w_{k+1} + h}{2}$	$\frac{w_{k-1} + w_k - w_{k+1} - h}{2}$
γ_k	$\pi i - w_k$	$\pi i - w_k$	$\pi i - w_k$	$\pi i - w_k$

The parametrization chosen here automatically satisfies the gluing condition for each

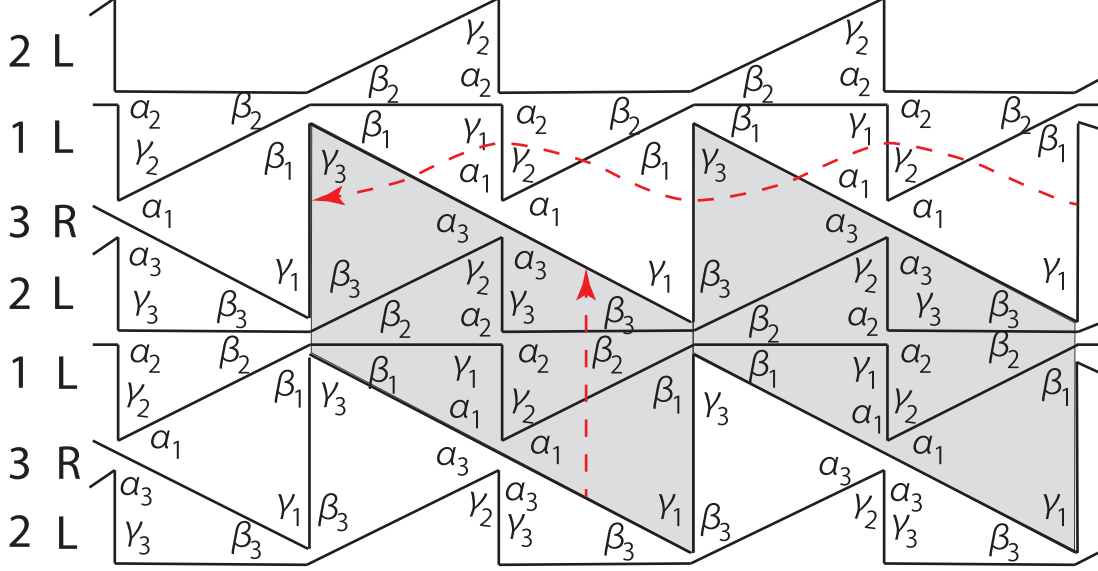


Figure 3: The figure for the boundary torus, for an example $\varphi = L^2 R$. The fundamental region of the torus is shown in gray. We express φ as a product of L and R , and we layer the four triangles of Figure 2 in different ways depending L or R . The angles in the figure are not depicted correctly, and angles with the same symbol should really be the same. A more complicated example can be found in Figure 4 of [17].

edge [17]. In the example of Figure 3, the consistency conditions are

$$2(\beta_1 + \beta_2 + \beta_3) + \gamma_1 + \gamma_3 = 2\pi i, \quad 2\alpha_2 + \gamma_1 + \gamma_3 = 2\pi i, \quad 2(\alpha_1 + \alpha_3 + \gamma_2) = 2\pi i.$$

This is satisfied by the parametrization

$$\begin{aligned} \alpha_1 &= \frac{-w_3 + w_1 + w_2 + h}{2}, & \alpha_2 &= \frac{w_1 + w_3}{2}, & \alpha_3 &= \frac{w_2 + w_3 - w_1 - h}{2}, \\ \beta_1 &= \frac{w_3 + w_1 - w_2 - h}{2}, & \beta_2 &= \frac{-w_1 + 2w_2 - w_3}{2}, & \beta_3 &= \frac{-w_2 + w_3 + w_1 + h}{2}, \\ \gamma_1 &= \pi i - w_1, & \gamma_2 &= \pi i - w_2, & \gamma_3 &= \pi i - w_3. \end{aligned}$$

We still have to worry about the consistency conditions inside each tetrahedron; the three shape parameters in the same ideal tetrahedron must have relations

$$e^{-\alpha_k} = 1 - e^{\gamma_k}, \quad e^{-\beta_k} = \frac{1}{1 - e^{-\gamma_k}}. \quad (3.47)$$

Note that these two equations are not independent since we have $e^{\alpha_k + \beta_k + \gamma_k} = 1$. Since each of $\alpha_k, \beta_k, \gamma_k$ are written by w_{k-1}, w_k and w_{k+1} , these are relations among the variables w_k 's.

We can construct a potential $V_{\text{geom}}(w)$ whose derivative with respect to w_k reproduces (3.47). By extremizing the potential we find the complete hyperbolic structure on the mapping torus [11].

In the following we denote w_k by x_k, y_k , depending on whether the corresponding tetrahedron is L or R . Then the structure equations (3.47) will take the following form, depending whether each of $\Delta_{k-1}, \Delta_k, \Delta_{k+1}$ is of type L or R .

1. $(\Delta_{k-1}, \Delta_k, \Delta_{k+1}) = (L, L, L)$.

Following the rule in Table 1, we have

$$\alpha_k = \frac{w_{k-1} + w_{k+1}}{2}, \quad \beta_k = \frac{2w_k - w_{k-1} - w_{k+1}}{2}, \quad \gamma_k = i\pi - w_k. \quad (3.48)$$

We also have

$$x_j = w_j \quad (j = k-1, k, k+1). \quad (3.49)$$

From these equations the second equation of (3.47) becomes

$$\frac{1}{1 + e^{x_k}} = e^{\frac{1}{2}(-2x_k + x_{k+1} + x_{k-1})}. \quad (3.50)$$

This is reproduced from a potential

$$V_{\text{geom}}(x, y; h) \equiv -\text{Li}_2(-e^{x_k}) + \frac{1}{4}(-2x_k^2) + \frac{1}{2}x_k(x_{k+1} + x_{k-1}), \quad (3.51)$$

which coincides with the $V_{\text{trace}}(x, y; h)$.

The remaining cases are treated similarly, and we list the structure equation as well as the potential which reproduces it. Note that the structure equation itself is determined from Δ_{k-1} and Δ_k , and the L/R type of Δ_{k+1} changes only the label of the variable.

2. $(\Delta_{k-1}, \Delta_k, \Delta_{k+1}) = (L, L, R)$.

$$\frac{1}{1 + e^{x_k}} = e^{\frac{1}{2}(-2x_k + y_{k+1} + x_{k-1})}, \quad V_{\text{geom}} \equiv -\text{Li}_2(-e^{x_k}) + \frac{1}{4}(-2x_k^2) + \frac{1}{2}x_k(y_{k+1} + x_{k-1}).$$

3. $(\Delta_{k-1}, \Delta_k, \Delta_{k+1}) = (R, L, L)$.

$$\frac{1}{1 + e^{x_k}} = e^{\frac{1}{2}(-x_k + x_{k+1} - y_{k-1} + h)}, \quad V_{\text{geom}} \equiv -\text{Li}_2(-e^{x_k}) + \frac{1}{4}(-x_k^2) + \frac{1}{2}x_k(x_{k+1} - y_{k-1}) + \frac{h}{2}x_k.$$

$$4. (\Delta_{k-1}, \Delta_k, \Delta_{k+1}) = (R, L, R).$$

$$\frac{1}{1+e^{x_k}} = e^{\frac{1}{2}(-x_k+y_{k+1}-y_{k-1}+h)}, \quad V_{\text{geom}} \equiv -\text{Li}_2(-e^{x_k}) + \frac{1}{4}(-x_k^2) + \frac{1}{2}x_k(y_{k+1}-y_{k-1}) + \frac{h}{2}x_k.$$

$$5. (\Delta_{k-1}, \Delta_k, \Delta_{k+1}) = (R, R, R).$$

$$\frac{1}{1+e^{y_k}} = e^{\frac{1}{2}(-y_{k+1}-y_{k-1})}, \quad V_{\text{geom}} \equiv -\text{Li}_2(-e^{y_k}) + \frac{1}{2}y_k(-y_{k+1}-y_{k-1}).$$

$$6. (\Delta_{k-1}, \Delta_k, \Delta_{k+1}) = (R, R, L).$$

$$\frac{1}{1+e^{y_k}} = e^{\frac{1}{2}(-x_{k+1}-y_{k-1})}, \quad V_{\text{geom}} \equiv -\text{Li}_2(-e^{y_k}) + \frac{1}{2}y_k(-x_{k+1}-y_{k-1}).$$

$$7. (\Delta_{k-1}, \Delta_k, \Delta_{k+1}) = (L, R, R).$$

$$\frac{1}{1+e^{y_k}} = e^{\frac{1}{2}(-y_{k+1}+x_{k-1}-y_k-h)}, \quad V_{\text{geom}} \equiv -\text{Li}_2(-e^{y_k}) + \frac{1}{4}(-y_k^2) + \frac{1}{2}y_k(-y_{k+1}+x_{k-1}) - \frac{h}{2}y_k.$$

$$8. (\Delta_{k-1}, \Delta_k, \Delta_{k+1}) = (L, R, L).$$

$$\frac{1}{1+e^{y_k}} = e^{\frac{1}{2}(-x_{k+1}+x_{k-1}-y_k-h)}, \quad V_{\text{geom}} \equiv -\text{Li}_2(-e^{y_k}) + \frac{1}{4}(-y_k^2) + \frac{1}{2}y_k(-x_{k+1}+x_{k-1}) - \frac{h}{2}y_k.$$

By comparing these results with the results in section 3.3, we have (up to constant terms)

$$V_{\text{trace}}(x, y; h) = V_{\text{geom}}(x, y; h), \quad (3.52)$$

where we used an identity of the classical dilogarithm (A.4). This is what we wanted to show. This equation demonstrates an equivalence of the potential *before extremization*, and clarifies the geometrical meaning of Fock variables x_k, y_k in hyperbolic geometry. Moreover, explicit computations show that, for all the 8 cases,

$$\text{Im} \left(V_{\text{trace}}(x, y, ; h) \Big|_{h=0} \right) = \sum_k D(e^{\gamma_k}) + \sum_k \text{Re}(w_k) \text{Im} \left(\frac{\partial V}{\partial w_k} \right), \quad (3.53)$$

where $D(z)$, the Bloch-Wigner function defined in (B.5), is the hyperbolic volume of an ideal tetrahedron with modulus z . This shows that the V_{trace} at the critical point gives precisely the hyperbolic volume of the 3-manifold.

We can also identify longitude and meridian parameters. The parameter h is identified

with \mathfrak{l} , and the expression inside the bracket of (3.46) coincides with a holonomy of a cycle along the boundary torus. For example, in Figure 3, the holonomy along the vertical direction gives

$$\mathfrak{m} = \alpha_1 - \beta_2 - \beta_3 = \frac{-w_1 + w_3}{2} = \frac{x_1 - y_3}{2},$$

whereas the one along the horizontal direction is

$$\mathfrak{l} = -\gamma_3 + (\alpha_1 + \gamma_2) - \beta_1 + i\pi = h + i\pi.$$

The general proof can be given similarly. Note meridian parameter \mathfrak{l} is given as an \hbar -linear term in the potential of the quantum Teichmüller theory, and does not require extra input — this is in sharp contrast with the state sum model of [19], where the longitude constraint is put in by hand as a delta function.

4 Concluding Remarks

In this paper we have demonstrated that the classical limit of the partition functions of 3d theory gives the hyperbolic volume (and Chern-Simons invariant) of the 3-manifold, in the case of the once-punctured torus.

It would be interesting to extend the discussion to a more general Riemann surface, and to discuss perturbative corrections to the volume (see [20, 21, 22]).

Acknowledgments

The content of this paper was presented by M. Y. at the String-Math 2011 conference (University of Pennsylvania, June 2011), and we thank the audience for feedback. Y. T. is supported in part by the Grants-in-Aid for Scientific Research, JSPS. M. Y. thanks PCTS for its support. We would like to thank T. Dimofte, H. Fuji, D. Gaiotto, T. Nishioka and Y. Tachikawa for discussion.

A Quantum Dilogarithm

In this appendix we collect formulas for the non-compact quantum dilogarithm function $e_b(z)$ [23, 24, 25].

The function $e_b(z)$ is defined by

$$e_b(z) = \exp \left(\frac{1}{4} \int_{-\infty+i0}^{\infty+i0} \frac{dw}{w} \frac{e^{-i2zw}}{\sinh(wb) \sinh(w/b)} \right), \quad (\text{A.1})$$

where the integration contour is chosen above the pole $w = 0$, and we require $|\text{Im } z| < |\text{Im } c_b|$ for convergence at infinity. In the classical limit $b \rightarrow 0$, we have

$$e_b(z) \rightarrow \exp \left(\frac{1}{2\pi i b^2} \text{Li}_2(-e^{2\pi b z}) \right), \quad (\text{A.2})$$

where $\text{Li}_2(z)$ is the Euler classical dilogarithm function defined by

$$\text{Li}_2(z) = - \int_0^z \frac{\log(1-t)}{t} dt. \quad (\text{A.3})$$

This function satisfies

$$\text{Li}_2(-e^x) + \text{Li}_2(-e^{-x}) = -\frac{\pi^2}{6} - \frac{1}{2}x^2. \quad (\text{A.4})$$

After analytic continuation, $e_b(z)$ has a product expression when $\text{Im } b^2 > 0$:

$$e_b(z) = (e^{2\pi(z+iQ/2)b}; q^2)_\infty / (e^{2\pi(z-iQ/2)b^{-1}}; \bar{q}^2)_\infty, \quad (\text{A.5})$$

where $(x; q)_\infty$ is defined by

$$(x; q)_\infty = \prod_{n=1}^{\infty} (1 - xq^n), \quad (\text{A.6})$$

and $q := e^{i\pi b^2}$, $\bar{q} := e^{-i\pi b^{-2}}$. This implies

$$\begin{aligned} e_b(z - 2ib) &= (1 + q^{-1}e^{2\pi bz})(1 + q^{-3}e^{2\pi bz}) e_b(z), \\ e_b(z + 2ib) &= (1 + qe^{2\pi bz})^{-1}(1 + q^3e^{2\pi bz})^{-1} e_b(z). \end{aligned} \quad (\text{A.7})$$

B Rudiments of Hyperbolic Geometry

In this section we quickly summarize some basics facts of hyperbolic geometry needed for the understanding of this paper. See, for example, [26] for further introduction.

Let \mathbb{H}^3 be a 3d hyperbolic space, namely a upper half plane

$$\mathbb{R}_{>0}^3 = \{(x_1, x_2, y) \mid x_1, x_2 \in \mathbb{R}, y > 0\}, \quad (\text{B.1})$$

with the metric

$$ds^2 = \frac{(dx_1)^2 + (dx_2)^2 + dy^2}{y^2}. \quad (\text{B.2})$$

This has a boundary $\partial H^3 = \mathbb{C} \cup \{\infty\}$, and has isometry $PSL(2, \mathbb{C})$.

A hyperbolic manifold can be written in the form \mathbb{H}^3/Γ , where Γ is a torsion free discrete subgroup of $PSL(2, \mathbb{C})$. The examples discussed in this paper are knot complements. Suppose that we have a 3-manifold M , and a knot K inside. The knot complement of K inside M is a complement of the tubular neighborhood $N(K)$ of M

$$M \setminus K := M \setminus N(K). \quad (\text{B.3})$$

By construction the boundary of $M \setminus K$ is the boundary of $N(K)$, which is a torus. The cycle of the torus contractible (non-contractible) in $N(K)$ is called the meridian (longitude).

An ideal tetrahedron is a tetrahedron whose all four vertices are on the boundary of \mathbb{H}^3 (see Figure 4). By a suitable Möbius transformation we can take the vertices to be at positions $0, 1, z$ and infinity. This parameter z is called the modulus (shape parameter) of the tetrahedron.

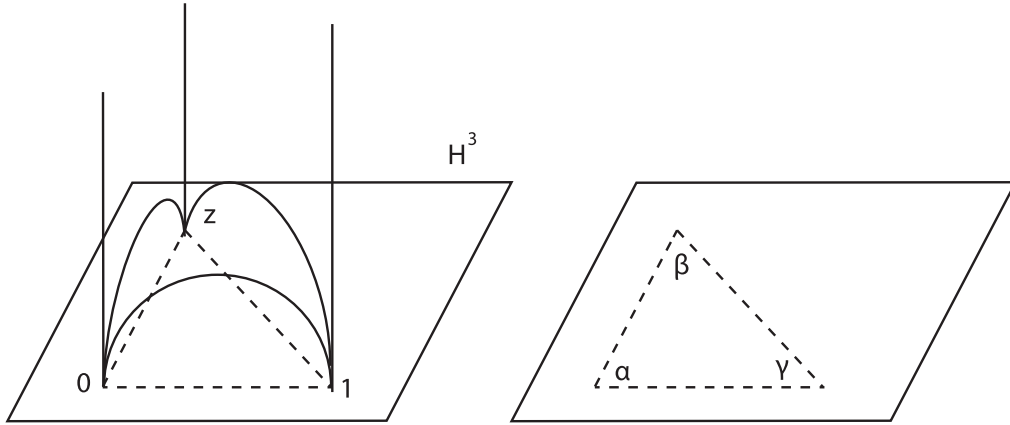


Figure 4: An ideal tetrahedron in \mathbb{H}^3 has all the four vertices on the boundary of \mathbb{H}^3 , which we can take to be $\{0, 1, z, \infty\} \in \mathbb{C} \cup \{\infty\}$.

A tetrahedron has 6 edges and correspondingly 6 face angles. For an ideal tetrahedron with modulus z , the two face angles on the opposite side of the tetrahedron are the same.

These are given as the arguments of three complex parameters

$$z = e^\alpha, \quad \frac{1}{1-z} = e^\beta, \quad 1 - z^{-1} = e^\gamma, \quad (\text{B.4})$$

satisfying $e^{\alpha+\beta+\gamma} = 1$ and the relations as in (3.47). The hyperbolic volume of an ideal tetrahedron with modulus z is given by the Bloch-Wigner function $D(z)$:

$$D(z) = \text{Im}(\text{Li}_2(z)) + \arg(1-z) \log|z|, \quad (\text{B.5})$$

which satisfies

$$D(z) = D(1 - z^{-1}) = D\left(\frac{1}{1-z}\right) = -D(z^{-1}) = -D(1-z) = -D\left(\frac{1}{1-z^{-1}}\right). \quad (\text{B.6})$$

Let us now glue the tetrahedron to construct 3-manifolds. There are two types of boundary conditions we need to impose. First, we need a gluing condition around an edge or the triangulation:

$$\prod_{\text{edge}} z_i = 1. \quad (\text{B.7})$$

This says that the angles around an edge sum up to 2π . This condition is already taken care of in the parametrization of [17] explained in the main text. There are also gluing conditions along the torus boundaries. This can be written as

$$\prod_{\text{meridian}} z_i = M, \quad \prod_{\text{longitude}} z_i = L^2. \quad (\text{B.8})$$

Here the two parameters M (L) are called meridian (longitude) parameters, and their logarithms are denoted by \mathfrak{m} (\mathfrak{l}). In Chern-Simons theory they are the holonomies along α and β -cycles.

$$\rho(\alpha) = \begin{pmatrix} M^{1/2} & * \\ 0 & M^{-1/2} \end{pmatrix}, \quad \rho(\beta) = \begin{pmatrix} L & * \\ 0 & L^{-1} \end{pmatrix}, \quad (\text{B.9})$$

If we take $M = 1$, we have a complete hyperbolic metric, and there are only isolated solutions of (B.7) and (B.8). The parameter M is a 1-parameter deformation of the hyperbolic structure [12].

References

- [1] Y. Terashima and M. Yamazaki, (2011), arXiv:1103.5748.
- [2] N. Drukker, D. Gaiotto, and J. Gomis, (2010), arXiv:1003.1112.
- [3] K. Hosomichi, S. Lee, and J. Park, (2010), arXiv:1009.0340.
- [4] L. F. Alday, D. Gaiotto, and Y. Tachikawa, Lett. Math. Phys. **91**, 167 (2010), arXiv:0906.3219.
- [5] D. Galakhov, A. Mironov, A. Morozov, and A. Smirnov, (2011), arXiv:1104.2589.
- [6] T. Dimofte, S. Gukov, and L. Hollands, (2010), arXiv:1006.0977.
- [7] A. Gadde, L. Rastelli, S. S. Razamat, and W. Yan, (2011), arXiv:1104.3850.
- [8] T. Nishioka, Y. Tachikawa, and M. Yamazaki, (2011), arXiv:1105.4390.
- [9] S. Gukov, Commun. Math. Phys. **255**, 577 (2005), arXiv:hep-th/0306165.
- [10] J.-P. Otal, Astérisque , x+159 (1996).
- [11] I. Rivin, Ann. of Math. (2) **139**, 553 (1994).
- [12] W. D. Neumann and D. Zagier, Topology **24**, 307 (1985).
- [13] D. Cooper, M. Culler, H. Gillet, D. D. Long, and P. B. Shalen, Invent. Math. **118**, 47 (1994).
- [14] E. Witten, Commun. Math. Phys. **121**, 351 (1989).
- [15] V. V. Fock and A. B. Goncharov, Ann. Sci. Éc. Norm. Supér. (4) **42**, 865 (2009).
- [16] W. Floyd and A. Hatcher, Topology Appl. **13**, 263 (1982).
- [17] F. Guéritaud, Geom. Topol. **10**, 1239 (2006), With an appendix by David Futer.
- [18] J. Porti, C. R. Acad. Sci. Paris Sér. I Math. **320**, 59 (1995).
- [19] K. Hikami, J. Geom. Phys. **57**, 1895 (2007).
- [20] R. Dijkgraaf and H. Fuji, Fortsch. Phys. **57**, 825 (2009), arXiv:0903.2084.

- [21] T. Dimofte, S. Gukov, J. Lenells, and D. Zagier, Commun. Num. Theor. Phys. **3**, 363 (2009), arXiv:0903.2472.
- [22] R. Dijkgraaf, H. Fuji, and M. Manabe, Nucl. Phys. **B849**, 166 (2011), arXiv:1010.4542.
- [23] L. Faddeev and A. Y. Volkov, Phys. Lett. B **315**, 311 (1993).
- [24] L. D. Faddeev and R. M. Kashaev, Modern Phys. Lett. A **9**, 427 (1994).
- [25] L. D. Faddeev, Lett. Math. Phys. **34**, 249 (1995), arXiv:hep-th/9504111.
- [26] W. P. Thurston, Bull. Amer. Math. Soc. (N.S.) **6**, 357 (1982).